Performance Analysis of a Tri-adjustable Automated Heavy-Duty Handling System Designed on Industry 4.0 Principles

S.Z. Mafokwane

Department of Mechanical and Industrial Engineering Technology
University of Johannesburg
Johannesburg, South Africa

zamashaun@gmail.com

Daramy Vandi Von Kallon
Department of Mechanical and Industrial Engineering Technology
University of Johannesburg
Johannesburg, South Africa
dkallon@uj.ac.za

Abstract

Over the years, many South African industries have been using Forklift trucks to move bigger loads from one point to another till today. The use of large forklift trucks within indoor manufacturing processes poses OHS risks to workers as its Internal Combustion Engine (ICE) produces fumes (Carbon Monoxide, CO) when in operation and exhaust fumes, (CO), are harmful to human's health. On this basis, a new system design is recommended to eliminate the use of MHS that relies on ICE power source to prevent OHS risks in indoor manufacturing industries. In this project, Autodesk Inventor Professional software was used for design development of technical drawings and simulation as well as validation of the new system's structure. Vehicle Dynamics' principles and equations are used to determine the overall Rolling Resistance, Tractive Effort of the new system, wheel torque, and the power required to drive the system under 20 – ton load capacity. The new system design has been developed to operate using a Hydraulic Power pack source, where it consists of four hydraulic wheel hubs for driving the system, four hydraulic cylinders for lifting & lowering, and a double rod end hydraulic cylinder for steering. Electro-Hydraulic circuit systems were developed and proposed using electronics and fluid mechanics phenomena. Again, principles, laws and equations of Strength of Materials has been carried out for validation of the material selection of the new design system's structure as well as verifying buckling, deflection & bending stresses, and moments.

Keywords: Material Handling System, Internal Combustion Engine, Occupational Health & Safety, Manufacturing, Hydraulics, Finite Element Methods.

1. Introduction

The aim of this document is to model and analyze the performance of the final design chosen for the design of a Tri-adjustable Automated Heavy-Duty Handling System based in Industry 4.0 principles. The design parameters of the selected concept, thus for the new system includes calculation & verification of Vehicle Dynamics of the new system, Stress Analysis of the main structure and hoisting mechanism, and Hydraulic Power pack validation in terms verifying operating pressures for the hydraulic system. Calculations of the new model were carried out in this chapter considering the different varying design parameters (Mainly SWL & Frame structure material) of the new system. The specification of the new design system should be accurate to achieve the correct results and/or outcomes for safe operation and proper handling of goods in the workplace (Mafokwane, at el., 2019).

2. Technical Calculations of the New System Design

This section focuses on verifying and validating the new system's stability, and performance. Whereby the overall system, based on material and components selected to form the new design, must be able to lift, lower and be able to move even when under maximum load. Therefore, engineering principles, laws and equation are carried out is achieving.

3. Vehicle Dynamics Approach

This section provides analysis and study of how the new system will react to driver inputs on a given road or surface condition. Vehicle motions are largely due to the shear forces generated between the tires and road, and therefore the tire model is an essential part of the mathematical model. In this paper the tire model will be analyzed to produce realistic shear forces during braking, acceleration, cornering, and combinations, on a range of surface conditions. As shown in Figure 1 (ONE n.d.).

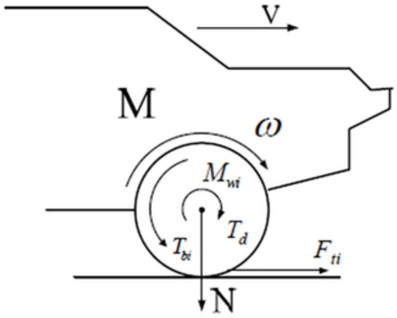

Figure 1 - Quarter model of vehicle expressing wheel and body dynamics (ONE, n.d.).

When selecting drive wheel motors for mobile vehicles, several vehicle dynamics factors are considered to determine the maximum torque required to move the vehicle. To choose motors capable of producing enough torque to propel the new proposed system, it is necessary to determine the total tractive effort (TTE) requirement for the vehicle (Mafokwane, 2021):
TTE [N] = RR [N] + Fa [N] …………………………………………………………………… (1)
The components of this equation will be determined in the following steps below.

3.1. Determining Rolling Resistance

Rolling Resistance (RR) is the force necessary to propel a vehicle over a surface. The worst possible surface type to be encountered by the vehicle will be factored into the equation (Mafokwane, at el., 2019).
RR[N] = W_GV [N]+μ ………………………………………………………………... (2)
Therefore:
Considering worst possible surface type and maximum load capacity condition to achieve RR of the new system.
W_GV = 30000×9.81 = **294.3 kN** ; μ=0.71 (as shown in table 13)
RR = 294300×0.71 = **208.953 kN**

3.2. Determining Acceleration Force

Acceleration Force (Fa) is the force necessary to accelerate from a stop to maximum speed in a desired time.

$Fa = \frac{W_{GV} \times V_{max}}{g \times t_a}$ ………………………………………………………………………….. (3)
Calculation data.
Considering, $t_a = 1s$; $V_{max} = 5\frac{km}{hr}$ $(walking\ speed)$; $g = 9.81[\frac{m}{s^2}]$
$W_{GV} = 294{,}3\ kN$ to achieve Fa of the new system.

$$Fa = \frac{294{,}3 \times {}^{5}/_{3600}}{9.81 \times 1} = \mathbf{41.67\ kN}$$

3.3. Determining Total Tractive Effort

The Total Tractive Effort (TTE) is the sum of the forces calculated in 3.1. and 3.2.
Therefore: TTE[N]=RR [N]+Fa[N] (as shown in equation 1)

TTE = 208,953+41.67 = **250.623 kN**

3.4. Determining Hydraulic Wheel Motor Torque

To verify if the new proposed system will perform as designed with regards to tractive effort and acceleration, it is necessary to calculate the required wheel torque (T_w) based on the tractive effort.

$$T_w = TTE \times R_w \times R_f \quad \ldots \quad (4)$$

The resistance factor accounts for the frictional losses between the solid pneumatic tires and the drag on their hydraulic drive hub gear system and bearings. Typical values range between 1.1 and 1.15 (or 10 to 15%) (Joseph E. Shigley, 1996).

Considering, $R_f = 1.1$; $R_w = 0.541\ m$; $TTE = 250.623\ [N]$

$$T_w = 250.623 \times 0.541 \times 1.1 = 149.1\ kN.m$$

3.5. Determining Bending Moments of System Frame Structure

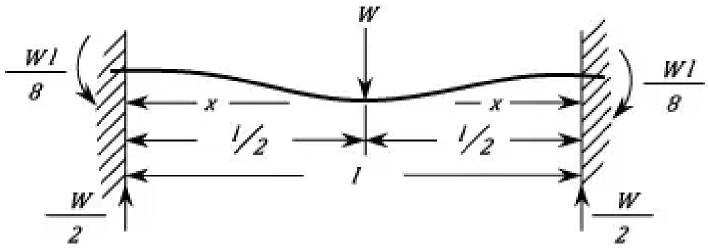

Figure 2 - Fixed End Moments structure diagram (Quora, n.d.).

Please note, only a quarter of the system is analyzed (Figure 2) because each quarter exert the same force as 20 ton of load is uniformly distributed, Figures 3 and 4 (Mafokwane, at el., 2019). Therefore,

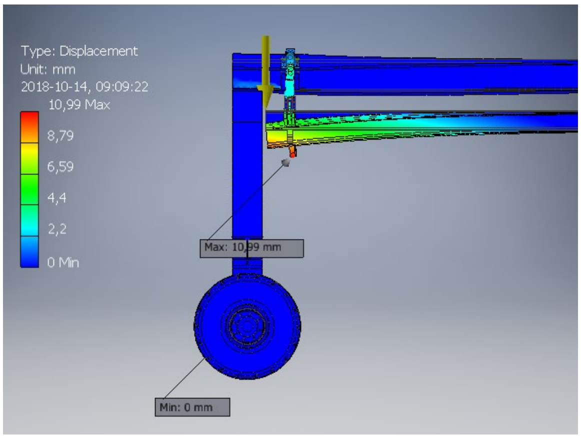

Figure 3 - New system Quarter Section illustration under load (Mafokwane, at el., 2019).

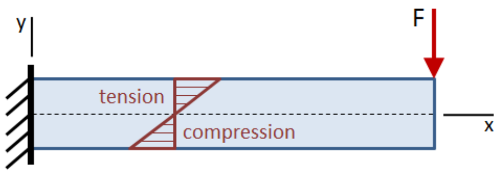

Figure 4 - Cantilever Free body diagram (MechaniCalc, n.d.).

Bending stress of the spreader beam.

$\sigma = \frac{BM}{I_x}$ (as shown in equation 4) σ = (49.05×0.3× 〖10〗^3)/(47.8× 〖10〗^(-6)) = **307.845 MPa (safe)**

SABS 1431 EN10025 Standard H-sectioned steel, Ultimate Tensile Stress 480 – 650 MPa, Yield strength 340-350 MPa, BHN Hardness average 140, with good LH practice weldability. Safety Factor, n= 650/307.845 = 2.11, good safety factor for heavy duty handling (Mafokwane, at el., 2019).

4. Shear Stress for H-Section Beam

The Shearing Force at any cross section of a Beam will set up a Shear Strain on transverse sections which in general will vary across the section.

In the following analysis it has been assumed that the Stress is uniform cross the width (i.e., parallel to the neutral axis) and that the presence of shear stress does not affect the distribution of Bending Stress. Due to the Shear Stress on transverse planes, there will be complementary planes parallel to the neutral axis, Figure 5 (Joseph E. Shigley, 1996).

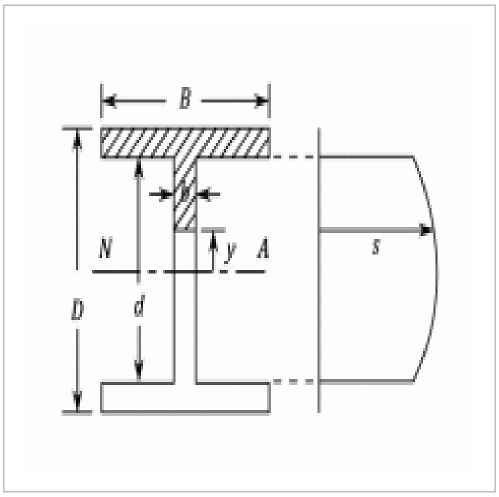

Figure 5 - Standard steel section shear distribution diagram (MechaniCalc, n.d.).

V: Shear Force

I_x: Moment of Inertia

I: Second area moment of the cross-section

B: Thickness of the material

Shear Stress calculation data.

The shear stress from A-A: $\tau_A = 0$, (A=0)

$V = 6000x9.81$

$V = 58.86kN$

$I_x = 195x10^{-6}m^4$

$$\bar{y}_{max} = \frac{356}{2} = 178mm \text{ (from botom)}$$

$$\tau_{max} = \frac{VA\bar{y}}{IB}$$

The shear stress from B-B:

$$\tau_B = \frac{VA\bar{y}}{Ib} \quad \ldots\ldots\ldots\ldots\ldots\ldots\ldots\ldots\ldots\ldots\ldots\ldots\ldots\ldots\ldots\ldots\ldots\ldots\ldots\ldots \quad (5)$$

$$\tau_B = \frac{(58.86x10^3)(9.1x10^{-3}x0.171)(0.178 - \frac{0.0091}{2})}{(195x10^{-6})(0.171)}$$

$\tau_B = 2.786MPa$

The shear stress at the Neutral Axis:

$$\tau_{N.A} = \frac{VA\bar{y}}{Ib}$$

$$\bar{y} = (9.1x10^{-3}x0.171)\left(0.178 - \frac{0.00091}{2}\right) + (0.1689)(0.0157)(0.08445)$$

$$\bar{y} = 4.94x10^{-4}\mathrm{m}$$

$$\tau_{N.A} = \frac{(58.86x10^{3})(4.94x10^{-4})(9.1x10^{-3})}{(0.0157)(195x10^{-6})}$$

$\tau_B = 9.498\mathrm{MPa}$ ***(Safe for load type application)***

The maximum value of shear stress occurs at the neutral axis ($y_1 = 0$), and the minimum value of shear stress in the web occurs at the outer fibres of the web where it intersects the flanges:

$y_1 = \frac{\pm h_w}{2}$; .... (6)

Showing that the Shear Stress in the flanges varies from a maximum at the top web to zero at the outer tips.

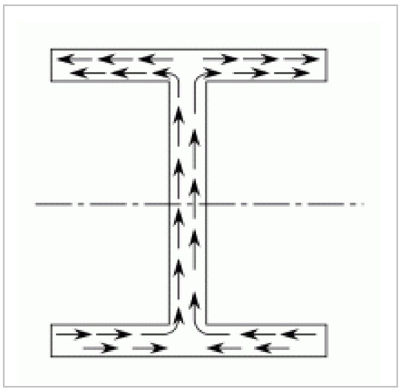

Figure 6 - H-beam stress distribution illustration [6].

The maximum deflection of this cantilever beam with end point load is found @ x=L and the maximum speed is found when the load @ x=L The distribution of shear stress along the web of an H-Beam is shown in Figure 6 and 7:

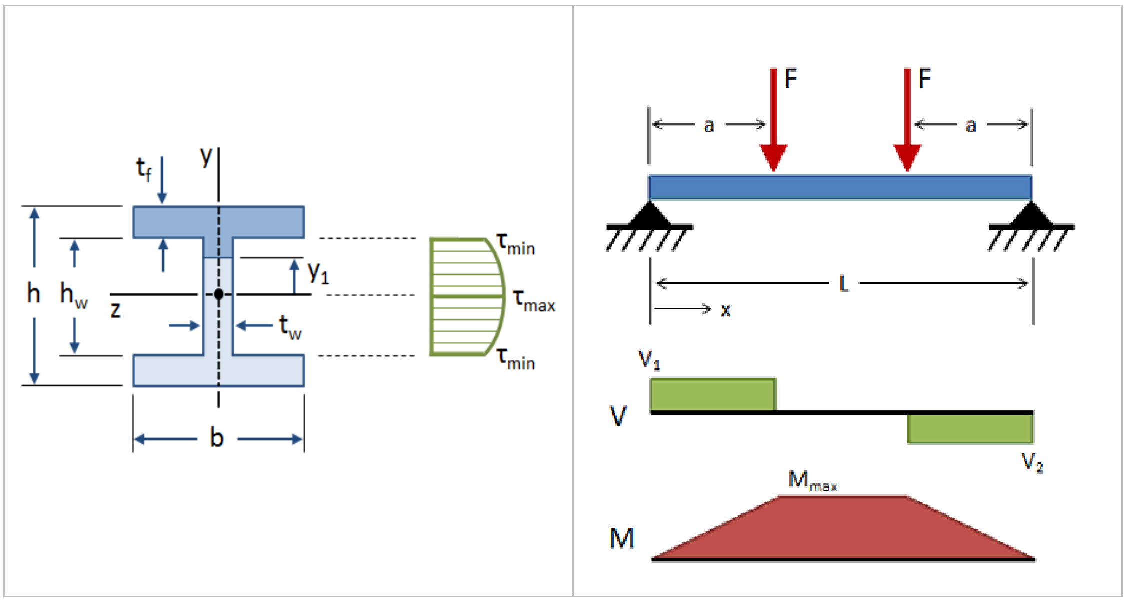

Figure 7 - Shear and Bending stress illustration on system structure.

5. Inside and Outside Steering Angle of the New Design System

The requirement for our vehicle is to keep turning radius low (Figure 8), so the outside turning radius of our vehicle was found to be 7.85 meters through vehicle dynamics technical calculations.

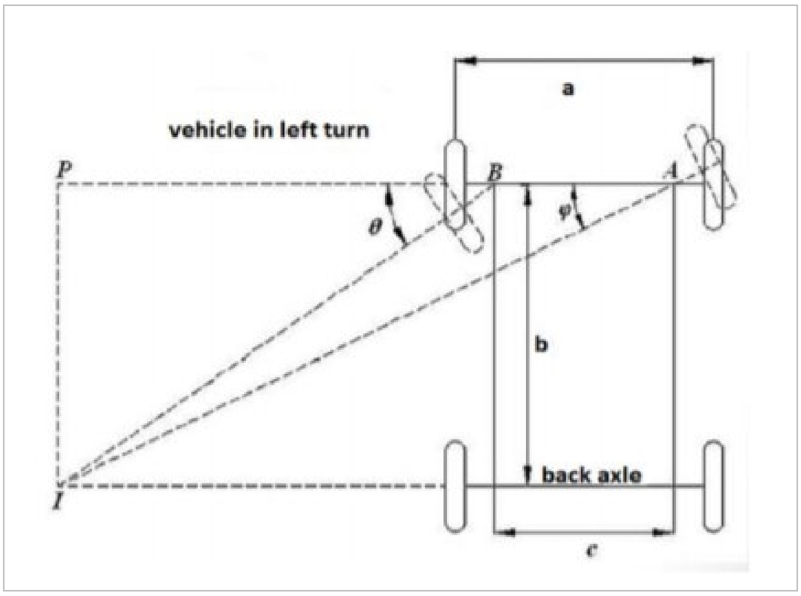

Figure 8 - Vehicle in turn IA is turning radius (Mafokwane, at el., 2019).

Therefore, Inside and Outside Steering Angle equation and calculation are as follows,

$R = \frac{b}{\sin\theta} + \frac{a-c}{2}$ [2,3] ………………....…………………………………………..….. (7)

(by geometry in Figure 8) in relation to a, b & c values that are dimensions of the new design system from Figure 8.

$7850 = \frac{4450}{\sin\theta} + \frac{3950-2730}{2},$

$\theta = \sin^{-1}(0.614)$

$\theta = 37.93°$

Now by correct steering geometry,

$\cot\theta - \cot\varphi = \frac{c}{b}$ [2,3] ……………..…………………………………………………. (8)

$\cot 37.93° - \cot\varphi = \frac{2730}{4450}$

$\varphi = \cot^{-1}(\cot 37.93° - \frac{2730}{4450})$

$\varphi = 56.2°$

Total steering angle = 37.93 + 56.2 = 94.13°

5.1. Determination of Steering Effort of the New Design System

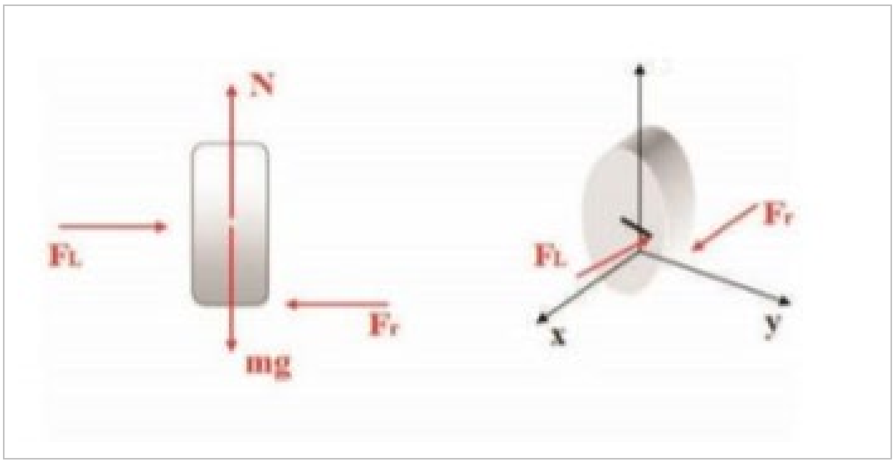

Figure 9 - Forces acting on wheel [4].

Referring to figure 9, forces acting on wheel variables' data description.

$\boldsymbol{mg}$: $Weight$

$\boldsymbol{F_L}$: $Lateral\ force$

$\boldsymbol{F_r}$: $Friction\ force$

N: $Normal\ force$

Steering effort is defined as the effort to be made by the driver or operator of a vehicle in turning the steering wheel. This can be calculated in either static condition i.e. when the vehicle is stationary and in dynamic conditions. Steering effort is maximum when the vehicle is stationary and the forces in all direction are in equilibrium (Mafokwane, at el., 2019).

W_GV = 30000×9.81 = **294,3 kN** (as shown in 4.2.2)

RA= RA= 1962002/= **98100** N (as shown in 3.3.3)

Reaction at each tire = $(RA/2\ +\ mass\ of\ tire) * 9.81$ ……………………..………………………….. (9)

$$= 98100/2 + 13.14 * 9.81$$

$$= \mathbf{481.31}\ kN$$

The tires used for the vehicle are mud tires and coefficient of friction between tires and rolled gravel ground is 0.6 (data provided by various tire manufacturers), as shown in Table 1.

Table 1 - Traction Coefficients for normal Vehicle Tires.

Surface	Traction Coefficient - μ_t -
Wet Ice	0.1
Dry Ice/Snow	0.2
Loose Sand	0.3 - 0.4
Dry Clay	0.5 - 0.6
Wet rolled Gravel	0.3 - 0.5
Dry rolled Gravel	0.6 - 0.7
Wet Asphalt	0.6
Wet Concrete	0.6
Dry Asphalt	0.9
Dry Concrete	0.9

The friction force at the tire is $= \mu * Reaction\ force\ at\ each\ tire$ ………………………………………. (10)

$$= 0.6 * 481.31 \times 10^3$$

$$= \mathbf{288.786}\ kN$$

While turning the steering wheel the torque will transmit to steering clamp bracket and then to the split joint shaft and this torque should be equal or greater than the frictional resistance of the ground to be able to turn the tire. From this, the value of steering arm torque is calculated by multiplying length of steering clamp bracket (460mm) with the friction force FR (Mafokwane, at el., 2019).

Steering Clamp Bracket (SCB) torque = $288.786 \times 10^3 \times 0.460$ = **132.84** kN-m

The amount of force or effort required on the steering wheel is calculated by dividing the torque by the radius of steering wheel (R = 945/2 mm) (Mafokwane, at el., 2019).

Therefore,

$$Steering\ effort\ =\ 132.84/\ (0.477)$$

$$Steering\ effort\ =\ \mathbf{278.49}\ kN$$

The amount of steering bending moment required on the steering clamp support bracket is calculated by multiplying the steering effort by the distance of the steering clamp bracket (Mafokwane, at el., 2019).

Therefore, steering clamp support bracket distance = 460 mm

$$Steering\ Bending\ Moment = 278.49 \times 0.46$$

$$= \mathbf{128.1}\ kN.m$$

5.2. Required Angle at the time of Maximum Turn

Table 2 - Required Internal Wheel Steer Angle at sharp corners (Mafokwane, at el., 2019).

Velocity (m/s)	FYF (N)	Slip Angle (degree)	Required angle (degrees)
0	0	0	0
1.39	67.23	0.16	54
2.78	268.9	0.7	53.4
4.167	602.2	1.5	52.67
5.55	1071.9	2.7	51.47
6.94	1700	3.96	50.21

Above table shows, that at the time of sharp cornering the vehicle is oversteering i.e., the rear tires lose their traction before front tires and slip angles are induced and required angle for maximum turning reduces because the vehicle is steering more than the operator or the driver’s feed at the steering wheel (Mafokwane, at el., 2019).

6. Design of the Hydraulic System of Working Device in the New Design System

6.1. Design Overview of the Hydraulic System

The new design system’ hydraulic system includes four lifting hydraulic cylinders and steering hydraulic cylinder. The lifting hydraulic cylinder can lift the goods. The Spreader Beam attached to lifting cylinders can make before and after loading framework, to facilitate handling and walking, and easy to use (Mafokwane, at el., 2019). The hydraulic pump’ output operational pressure creates hydraulic fluid flow into the working device and steering mechanism, respectively. A hydraulic system is an important power source of the working process of the new system design. A reasonable hydraulic system scheme can meet most requirements of various functions, and convenient manipulation, reliable operation, smooth motion, convenient adjustment, and maintenance of the new design system.

6.2. Principles of the Hydraulic System

Design description of the hydraulic power pack system:

- Hydraulic Tank,
- Hydraulic pump: the gear pump has been adopted as working oil pump,
- Working motor,
- Lifting oil cylinder: Double-acting hydraulic cylinder,
- Adjustable Hydraulic Steering Cylinder,
- Hydraulic control valve: multiple directional control valves,
- The speed limit flow control: a one-way valve,
- Auxiliary hydraulic parts design: design of filter, air filter design, various kinds of instrument choice selection of seal, hydraulic oil, and pressure loss calculation (Mafokwane, at el., 2019).

A) Maximum Working Pressure and Flow Rate of the Lifting Oil Cylinder

The working pressure is $100\ kg/cm^2$ & the flow rate is $50\ L/min$ for the system, thus normal pressure and flow rate for hydraulic heavy duty lifting systems (Mafokwane, at el., 2019).

B) Maximum Pressure of the Hydraulic System

Maximum pressure of the reversing valve requirement is $140\ kg/cm^2$, with reference to the similar products, P_1 has been chosen to be $100\ kg/cm^2$ (Mafokwane, at el., 2019).

6.3. Pump Power Capacity Analysis

Pump drive power validation,

$$P = \frac{P_p + Q_n}{61.2 \times \mu_v} \quad \text{(11)}$$

In the formula, P_p is the actual maximum working pressure of the pump, of 140 MPa; Q_n is the rated flow of pump and the operating value is $510\ m^3/s$; μ_v is the mechanical efficiency of the pump of 0.8 (Mafokwane, at el., 2019).

So, $P = \frac{140\times10^6 + 510\times10^{-6}}{61.2\times0.8}$

$P = \mathbf{1458.33}\ W$

6.4. Pump Motor Selection

Pump motor selection is conducted in accordance with the hydraulic pump rated speed and power needed to drive and deliver the rated flow rate. The Z4-112-4 electric motor has been selected and its parameters are as follows (Mafokwane, at el., 2019).

Table 3 - Pump Motor Specifications (Mafokwane, at el., 2019)

Rated power	5.5 kW
Rated voltage	160 V
Rated current	42.7 A
Speed (highest)	3000/4000 r/min
Efficiency	83.5%
Flywheel moment	0.8

So, pump motor' rated power calculation in relation to hydraulic pump power

$P = 1458.33\sqrt{\frac{15}{5}} = \mathbf{2525.9}\ W$, motor capable to run the hydraulic power pack system pump.

6.5. Design Calculation of the Tubing or Pipeline of the Hydraulic Power Pack System

Pressure & diameter of hydraulic power pack pipeline analysis:

$$Q = \frac{\pi}{4} \times d^2 \times v \quad \text{......} \quad (12)$$

Calculation data

$Q = 300\ L/min$; $v = 0.6\ m/s$

Therefore,

$$d = \sqrt{\frac{4 \times 300}{0.6 \times \pi}} = \mathbf{25.23}\ mm$$

Verifying the hydraulic system design manual, in accordance with the oil mouth nominal or fitting diameter size: d = 25 mm, outside diameter is 32 mm & the corresponding pipe fitting thread is M32×1.5 (Mafokwane, at el., 2019).

6.7. Velocity inside Hydraulic Tubing

$$V = \frac{4Q}{\pi d^2} \quad \text{......} \quad (13)$$

6.8. Wall Thickness of the Pipe Tubing

$$\delta = \frac{Pd}{2\,[\sigma]} \quad \text{......} \quad (14)$$

$$\delta = \frac{2100 \times 50}{2\,[1500]}$$

$$\delta = \mathbf{3.5}\ mm$$

The outside diameter of steel pipe tubing = $25 + 2 \times 3.5 = \mathbf{32}\ mm$

7. Fillet Weld Design

A flat-faced, equal-legged fillet weld in a 90° T-joint has a theoretical throat dimension of 0.707 ω, where ω is the leg size. When the welding process and procedure achieve a depth of penetration beyond the root, then the effective throat dimension is increased for fillet welds with equal leg sizes (Mafokwane, at el., 2019).

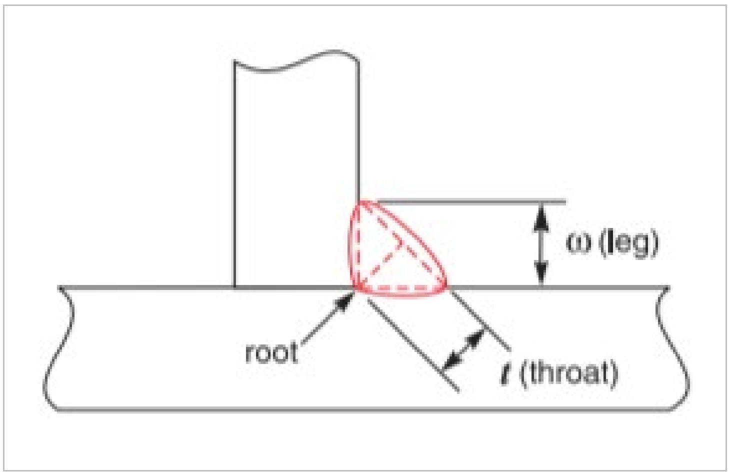

Figure 10 - Convex fillet weld (Mafokwane, at el., 2019).

7.1. Convex fillet weld – is a fillet weld in which the contour of the weld metal lies outside a straight line joining the toes of the weld. A convex fillet weld of specified leg length has a throat thickness more than the effective measurement.

Table 4 - Afrox Fillet and Weld Data.

Nominal Fillet Size (mm)	Min. Throat Thickness (mm)	Plate Thickness (mm)	Electrode Size (mm)
5,0	3,5	5,0 – 6,3	3,2
6,3	4,5	6,3 – 12,0	4,0
8,0	5,5	8,0 – 12,0 and over	5,0
10,0	7,0	10,0 and over	4,0

7.2. Front and Rear Wheel Hub Support Brackets weld summary

The new system design's hub support bracket materials have been chosen to be 40 mm thick plates. Available Carbon Steel plates available from the market ranges from 16 - 40 mm in thickness, therefore, for the design of hub bracket, thickest steel plate was chosen for over design purposes since the new system will be operating under heavy loads (20 – ton). Simulations of fabricated 40 mm thick steel plates will be simulated and evaluated in (Mafokwane and Kallon, 2019; Mafokwane and Kallon, 2020). Referring to Table 4, fabricated rear and front wheel hub support brackets have a Nominal fillet Size of 10.0 mm & Throat Thickness of 7.0 mm.

8. Conclusion

The research beacame a success whereby a new proposed MHS has been designed using Autodesk Inventor Professional and material selection of the new design system's components has been carried out and verified in relation with their strength & reliability properties. Through this paper and its engineering analysis, it is proven that the use of internal combustion engines in heavy duty handling systems that are operated within indoor manufactring factories and or internal logistics can be eliminated and replaced with an eco-friendly hydraulic systems technology. Therefore, this new system design promotes Occupational Health and Safety of people working in industrial areas where Bulk Material Handling systems are in place.

The new system was designed and it consist of four double-acting hydraulic cylinders interconnected with spreader beam responsible for lifting and lowering, as well as two double-acting hydraulic cylinders that will expand the system making it adjustable, a hydraulic steering cylinder for steering & turning the wheels and four hydraulic motors that will drive the system from point A to point B. Electric hydraulic components selection for new design system has been conducted.

Vehicle dynamics of the new proposed system were modelled, tested, and verified. The overall system's TE was calculated to discover the power required for the hydraulic wheel hub motor' to move the new proposed system under 20-ton load. When the new design system is under 20-ton load, TE was found to be 250.623 kN, hydraulic wheel hub motor torque was 149.1 kN.m and power required to overcome TE was 468.411 W, on each wheel.

References

Dr. V.K. Saini., May 2017. Design Methodology of Steering System for All-Terrain Vehicles. *International Research Journal of Engineering and Technology (IRJET),* 04(05), pp. 455-460.

Joseph E. Shigley., 1996. *Standard Handbook of Machine Design.* New York: McGraw-Hill.

Liai Pan, Q. D. a. C. H., 2015. *Design Research on Hydraulic System of Working Device of a Forklift.* China, s.n.

Manual,, n.d. *Welding Consumables - Carbon Steels.* [Online]
Available at: http://www.afrox.co.za/en/images/Section%2012%20-%20CarbSteel_tcm266-27348.pdf
[Accessed 18 September 2020].

MechaniCalc, n.d. *Bending Stresses & Deflections in Beams.* [Online]
Available at: https://mechanicalc.com/reference/beam-analysis
[Accessed 16 August 2020].

ONE, P., n.d. *Tire-road friction estimation and traction control strategy for motorized electric vehicle.* [Online]
Available at: https://journals.plos.org/plosone/article/figure?id=10.1371/journal.pone.0179526.g001
[Accessed 16 August 2020].

Quora, n.d. *What is fixed beam.* [Online]
Available at: https://www.quora.com/What-is-fixed-beam
[Accessed 16 August 2020].

ToolBox, E., 2010. *Factors of Safety.* [Online]
Available at: https://www.engineeringtoolbox.com/factors-safety-fos-d_1624.html
[Accessed 15 August 2020].

2017.

S.Z. Mafokwane,. Design of a Tri-Adjustable Automated Heavy-Duty \Handling System based on Industry 4.0 Principles. A Masters Dissertation submitted to the University of Johannesburg. 2021.

S.Z. Mafokwane, D.V.V. Kallon, M. Nkosi, F. Chiromo. Design of a Tri-Adjustable Automated Heavy Duty \Handling System based on Industry 4.0 Principles. *Procedia Manufacturing*. Volume 35, 2019. Pp 187 – 196.

S.Z. Mafokwane, D.V.V. Kallon. Hydraulic System Design of a Tri-Adjustable Automated Heavy-Duty Handling System Based On Industry 4.0 Principles. *2019 Open Innovations conference, OI 2019.* Pp. 420 – 424.

Mafokwane S.Z., Kallon D.V.V. Design of electro-hydraulic circuits for tri-adjustable automated heavy-duty industrial handling system. *Proceedings of the International Conference on Industrial Engineering and Operations Management. 2*020. 59. Pp 357 – 367.

Biographies

Shaun Zamawelase Mafokwane is a PhD candidate at the University of Johannesburg, Department of Mechanical and Industrial Engineering. Shaun is currently employed by Tetra Pak SA Pty Ltd and works as an Electro-Mechanical Service Engineer. He earned a National Diploma, a BTech degree, and MPhil in mechanical engineering from the University of Johannesburg. He is a member of the Institution of Certified Mechanical & Electrical Engineers and he is currently completing his GCC examination.

Dr Daramy Vandi Von Kallon is a Sierra Leonean holder of a PhD degree obtained from the University of Cape Town (UCT) in 2013. He holds a year-long experience as a Postdoctoral researcher at UCT. At the start of 2014 Dr Kallon was formally employed by the Centre for Minerals Research (CMR) at UCT as a Scientific Officer. In May 2014 Dr Kallon transferred to the University of Johannesburg as a full-time Lecturer and later a Senior Lecturer in the Department of Mechanical and Industrial Engineering Technology (DMIET). Dr Kallon has more than twelve (12) years of experience in research and six (6) years of teaching at University level, with industry-based collaborations. He is widely published, has supervised from master's to Postdoctoral and has graduated seven (7) Masters Candidates. Dr. Kallon's primary research areas are Acoustics Technologies, Mathematical Analysis and Optimization, Vibration Analysis, Water Research and Engineering Education.